THE EFFECT OF FAULT GOUGE ON FLUID FLOW, LISBON VALLEY, UT

BROADDUS, Carson L., Geosciences, Fort Lewis College, 1000 Rim Drive, Durango, CO 81301

Abstract

The existence of authigenic and reworked clays in fault zones is well understood to control the hydrologic and mechanical properties of faults. The net effect these clays have on fluid conductivity, reservoir quality, and fluid-derived mineralization is dependent on the origin of the gouge. To address this topic, I collected samples along four high-angle normal faults exposed within a copper mine in Lisbon Valley of Southeast Utah. The GTO, Lisbon Valley, Keystone, and Centennial faults were all sampled in gouge zones ranging from ~0.1 to ~5.5 meters across. Fault displacement ranged from 5 meters to 400 meters. Complementing field work was XRD analysis of all suitable samples to determine the quantity and type of clay in each gouge. We related the hydrologic properties affected by fault gouge with shale gouge ratio (SGR) and fault permeability computer modeling. SGR quantitatively estimates clay amounts in fault gouge that allow fault zone permeability estimates to be derived. Field interpretations suggest gouge zones are dominated by either maroon or green clays with most sites having lenses of the non-dominant component. Sampled gouge zones have grain sizes ranging from clay to fine sand and are poorly to moderately consolidated. Color of gouge samples does not seem to correlate with offset of faults, however, there is a correlation between grain-size and fault offset. XRD data shows high concentrations of illite and quartz in nearly all samples, and kaolinite present in samples with green/yellow hues. Modeling results predict high seal potential from SGR and very low permeability in nearly all sample sites. Understanding the effect on hydrologic dynamics will ultimately assist the team of geologists at the Lisbon Valley Mine further understand and predict copper mineralization along fault zones in the area along with constraints on fault-seal capacity when considering in-situ recovery.

Introduction

Clay minerals are commonly found in fault-produced rocks. These clays are most highly concentrated in faults zones with sedimentary components hosting a large gouge zone. Clay-dominated fault rocks are referred to as fault or clay gouge and are defined as tectonites with very fine grain size, consisting of mostly clay-sized particles. Fault gouges are well understood to affect fault hydrology, or the way fluids interact when encountering a fault surface. Along with water there is a suite of other economic fluids to account for such as migrating petroleum and mineral-rich hydrothermal fluids. The existence of clays in a fault core has been recognized to reduce permeability as much as seven orders of magnitude (Crawford et al., 2002; Davatzes et al., 2005). This reduction in conductivity leads to an inability of fluid passage across a fault zone. The occurrence of clay-rich fault gouge is the most influential factor on a fault's permeability and conductivity (Solum and van der Pluijm, 2009; Walsh et al., 1998, 2002).

Given the magnitude of influence that clay gouge has on fluid behavior, I attempted to quantify attributes of their concentrations and compositions. Understanding the composition used powder x-ray diffraction and Rietveld refinement modeling. This quantified the amount and type of clay minerals that are present within the gouge and assisted with model parameters as well as understanding the source of clays or enrichment of the gouge from surrounding stratigraphy. XRD data also assisted in developing an understanding of the genesis of clay gouge formation as it compares fluid alteration.

Another approach involved an empirical method of estimating clay concentrations and other fault zone properties through the application of modeling. One of the three methods to quantify fault gouge known as shale gouge ratio (SGR). SGR attempts to calculate clay concentrations based on the assumption that the gouge composition at a specified point is equivalent to the average composition of all the host rocks that has passed that point based on the throw of the fault. This implies that there was an equal mixing of all the different compositions up to that point in the stratigraphic section. Along with SGR, fault zone permeability and fault seal potential models were used to gain a better understanding of how fluids may interact with each fault.

This study focused on a few key faults in Lisbon Valley of southeast Utah. The faults in concern are all shallow, disconnected, high angle normal faults in all sedimentary hosts. The study sites include locations on the Lisbon Valley, Keystone, GTO, and Centennial faults. These faults vary in displacement from a few meters to a few hundred meters. The overall purpose of this study was to 1) describe and quantify the architecture, physical properties

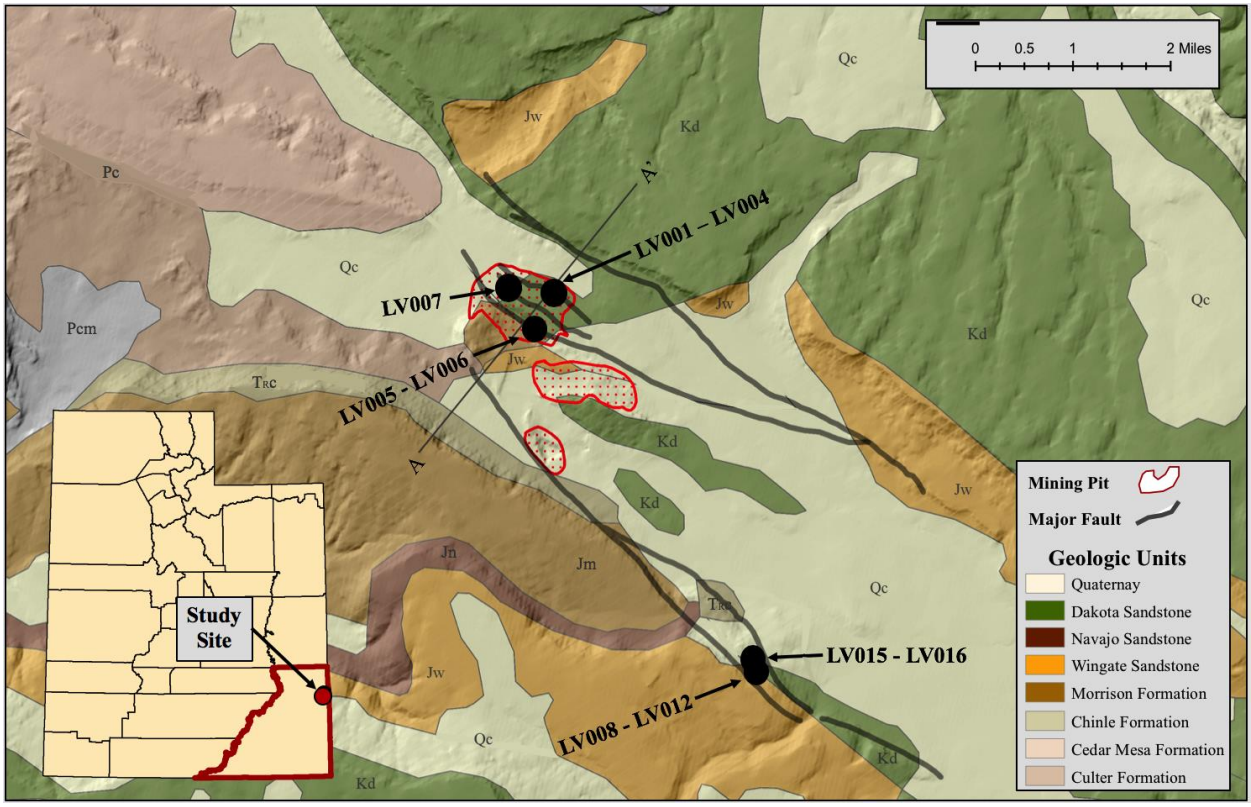

Fig. 1 – Regional and local location map of study area. Major faults in the region are represented as thick black lines. Surface geologic units displayed on top with sample site locations as dots.

and overall configuration of gouge zones; 2) quantify the mineralogy of the fault gouge in these zones; 3) model and predict the properties of these fault zones through the application of SGR, fault zone permeability, and fault seal potential models through computer software.

A major motivation for this project was to assist the Lisbon Valley Mine in understanding the dynamics of their subsurface geology. The mine is researching a recovery method known as in-situ recovery. This method involves injection of sulfuric acid into subsurface ore bodies to dissolve the copper into an acid solution. This acid is then pulled out of the ground and processed for the impregnated copper in solution. Performing this recovery requires an extremely developed understanding of subsurface flow. Understanding how fluids will act when encountering fault zones is a vital piece of this puzzle.

Background

Geologic Setting

Lisbon Valley, in southeastern Utah, is one of the many salt-cored anticlines of the Paradox Basin. The formation of these anticlines began in the late Paleozoic. Deposition of a sequence of Pennsylvanian evaporites, which filled the basin, was followed by fluvial clastic deposition from large scale fans sourced from the Uncompahgre Uplift (Leary et al., 2017). The creation of salt diapirs led to uplift through the late Pennsylvanian to the Triassic. This thick accumulation of salt deposits initially activated faults in the Early Mesozoic (Garden el al., 2001)(Fig 2). A lull in tectonism occurred until the Laramide Orogeny applied a northeast-southwest compressive stress (Garden el al., 2001). This stress caused growth of the anticlines of the Paradox, and the result is what we see today in Lisbon Valley (Garden el al., 2001). This compression around ~60 Ma also resulted in the reactivation and new

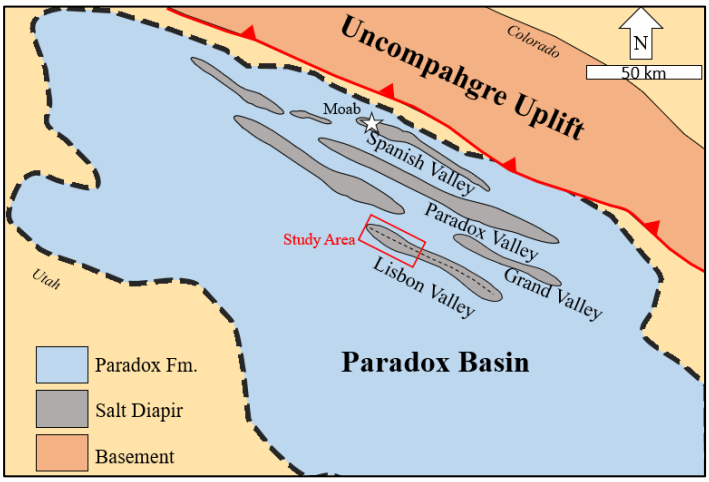

Fig. 2 – Regional map of Paradox Basin with salt valleys and study location in red box.

production of high-angle normal faults, typically striking north-northwest (Solum et al., 2005). Faults exposed at the surface in the Lisbon Valley (Lisbon Valley, GTO, Keystone, Centennial.) (Fig. 1) are now interpreted as shallow listric normal faults caused by a dissolution-induced collapse of the salt-cored anticline that underlies them. There are two types of faults in the valley; primary faults dipping to the NE and secondary or antithetic faults dipping to the SW. These faults and show a range of offsets. The major faults display offsets ranging from 100 meters to less than 10 meters while minor faults show at most 5 meters.

Fluid History

The fluid history of Lisbon Valley and the greater Paradox Basin has been a topic of discussion since research on the area began. In Lisbon Valley, there are extensive copper ore deposits, uranium and vanadium, and a producing oil field in the western part of the valley (Solum et al., 2010). This suite of geo-fluids has been interpreted in many ways and is still a topic of research today. The first fluids present in the valley are hydrocarbons sourced from the underlying Paradox Formation. As these hydrocarbons migrated upward around

120 Ma Fe^{3+} was reduced to Fe^{2+} and was mobilized (Beitler el al. 2003). This reduction of iron in the hematite caused the predominantly oxidized strata of Jurassic to be bleached and left in a reduced state. The reduced stratigraphy allowed for the next stage of fluids to oxidize and precipitate copper and uranium rich minerals in their place.

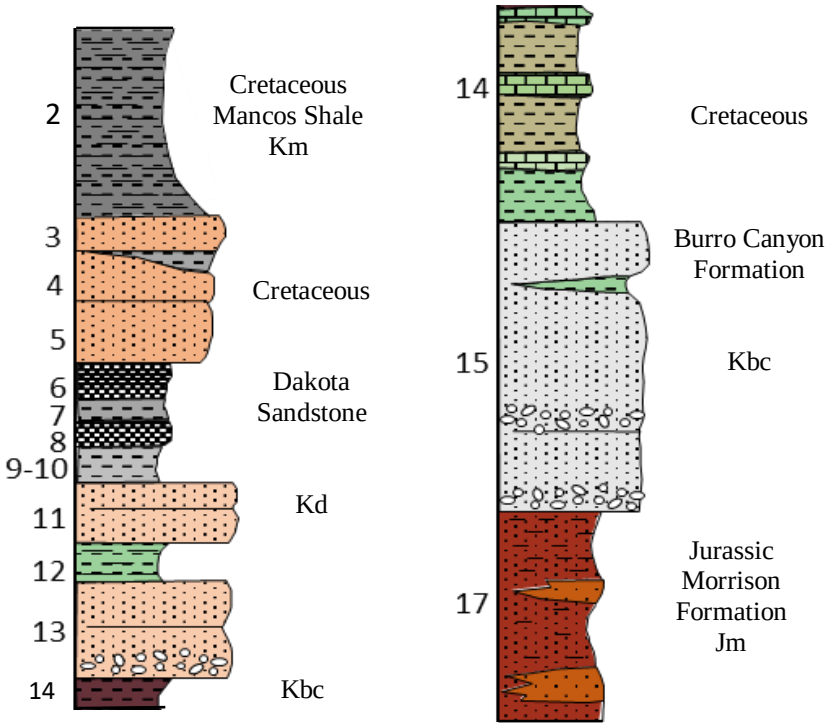

Fig. 3 – Stratigraphic section at Lisbon Valley Mine. Jurassic and Cretaceous strata that exposed in the various mining pits on the property. This section was designed by Brian Sparks and is property of the LVM.

Next in the story of fluid history was hydrothermal copper mineralization (Morrison and Parry, 1986). A variety of species exist within the valley, with the main ore minerals being chalcocite, chalcopyrite and many other minerals as products of alteration or secondary minerals. The intensity of the copper mineralization left an economically viable resource behind that has been mined since The Big Indian mine in 1903, with the largest and still active operation being the Lisbon Valley Copper Mine. The copper-bearing fluids migrated and were deposited near the faults within the valley; the age of copper mineralization remains unclear. Along with copper, dozens of other metals (including uranium and vanadium) were deposited in smaller quantities overall with high concentrations in localized sections of the valley (Morrison and Parry, 1986).

Stratigraphy

The exposed stratigraphy of Lisbon Valley is from Pennsylvanian to Cretaceous in age. The Paradox Formation (a sequence of evaporites) is the oldest stratigraphic unit in the area. The remaining section is composed of sequences of sandstones and shales from a range of depositional environments.

The Lisbon Valley mine has developed their own nomenclature for the local stratigraphy (Brian Sparks, personal communication). This nomenclature will be applied to this paper and referenced frequently

(Fig. 3). The stratigraphy in the pit is designated by bed number ranging from oldest (Morrison) Bed 17, to youngest (Quaternary Alluvium) Bed 1. The Burro Canyon Formation is divided into two beds, 15 and 14, both of which are 100 feet thick. Bed 15 is a pebbly fluvial conglomerate with packages of fining upward sequences representing a braided stream deposit. Bed 14 is a finer grained fluvial deposit with uniform distribution throughout. Beds 13-11 are the Lower Dakota Sandstone. Bed 13 is a fining upward immature sandstone ~35 feet thick, Bed 12 is a fine grain sandstone ~10 feet thick, and Bed 11 is a coarse to medium, fining upward package of sands that is ~20 feet thick. Beds 10-6 are all sequences of interbedded coarse to fine sands, shales, and coal beds within the Dakota, all from 10-30 feet in thickness. Beds 5-3 comprise the Upper Dakota and are all coarse to medium sandstones with fining upward sequences that have scoured bases into the sequence below, representative of migrating channel systems. Finally, Bed 2 is the undivided Mancos Formation that composes the top of the mining pits.

Faults

There are four major faults in Lisbon Valley along with several smaller antithetic faults, splays, and relays. These major faults are the result of salt tectonics sourced from the Paradox Formation. Salt can flow under load over geologic time, as sedimentation occurs on top of the salt, the salt begins to flow and create diapirs. A salt diapir is a dome or column-like feature similar to an anticline. These elongated domes cause extensive faulting of overlying stratigraphy into the salt. The current configuration of faults formed after the dissolution and collapse of the salt anticline. Millions of years of salt dissolution form meteoric or ground water fluids resulted in the collapse of the anticline. The faults created by this failure were high angle normal faults bounding the north and south flanks of the anticline as well as the associated antithetic faults.

Previous Work

Similar research has been conducted of fault gouge. A study by Solum (2010) investigated the timing and configuration of fault rocks along the Moab fault outside of Moab, Utah. Solum applied SGR and clay-smear potential models to conclude that as clay concentration increases, permeability of the fault zone decreases, and capillary entry pressure increases. This research was conducted in the Spanish Valley, which is a salt diapir in the same type of stratigraphy. Along with similar settings, a very similar fluid history has been interpreted. Overall, Solum's 2010 study has very valuable methodology and results to assist this research effort.

Methods

Field Sampling

Each sample taken from the five sites that were labeled with systematic names tied to the source location as well as a description of fault zone. Every sample was collected within the fault core specifically targeting gouge zones. Samples taken were selected based upon field observations of abundance, color and texture. Key traits observed were the apparent abundance of clay within a zone, unique in color or texture from surrounding zones, and thickness of the target zone. These attributes were chosen to achieve a diverse sample set. While many of these samples were already exposed due to the mining activity, samples from Lucky Strike were obtained by clearing and then digging a lateral trench across the exposure. Samples from the mine pit were taken in rapid succession while operations were halted, and pit access was granted. Collection at Lucky Strike (LV008-LV016) was methodical, and details were better recorded. The outer 10-20 cm of material exposed at the surface was removed from all sampling locations to ensure collected material was not altered by surface weathering processes.

Five distinct and separate sites were identified and chosen for sampling with a total of 16 samples collected. Three of these sites were within the active mining area (7 samples) and the remaining sites at Lucky Strike are naturally exposed fault zone east of the mining area where the following 9 samples were collected (Fig. 1).

Location one (Fig. 1 & Fig. 4) is an exposure along the East Centennial fault visible within the north side of active Centennial mining pit. The fault shows approximately 30 meters of offset here. This site has a roughly 1.5-meter thick zone of clay-rich gouge, sandwiched between heavily damaged outcrops

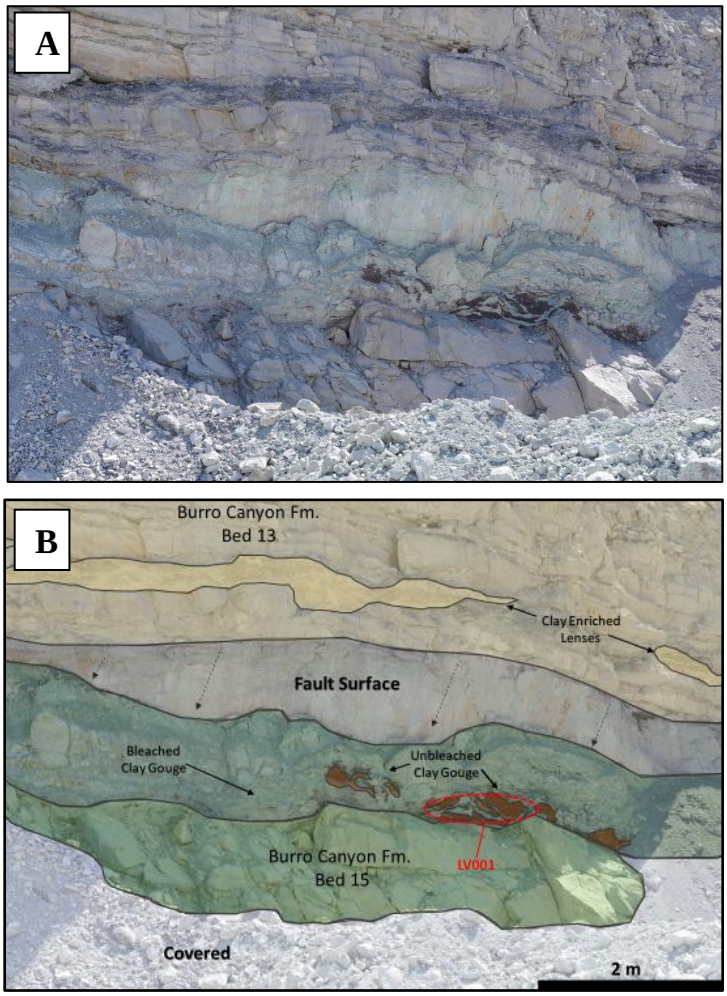

Fig. 4 – Sample site 1 within the active mining pit (LV001). Existence of both maroon and tan color gouge shown within near proximity to fault surface.

of Dakota Sandstone (Kd) in the hanging wall and lower Burro Canyon (Kbc) in the footwall. The gouge in this location has been bleached yellow/white with interbedded lenses of dark red unbleached gouge. Both unique gouge compositions were sampled separately. The most extensive damage surrounding the fault core extends ~ 5 meters in either direction with less intense alteration in the hanging wall than the footwall. One sample, LV001, was collected from this site.

Location two is located at the east side of the main active pit along the Lisbon Valley fault (LVF) (Fig. 5). At this site, the Navajo

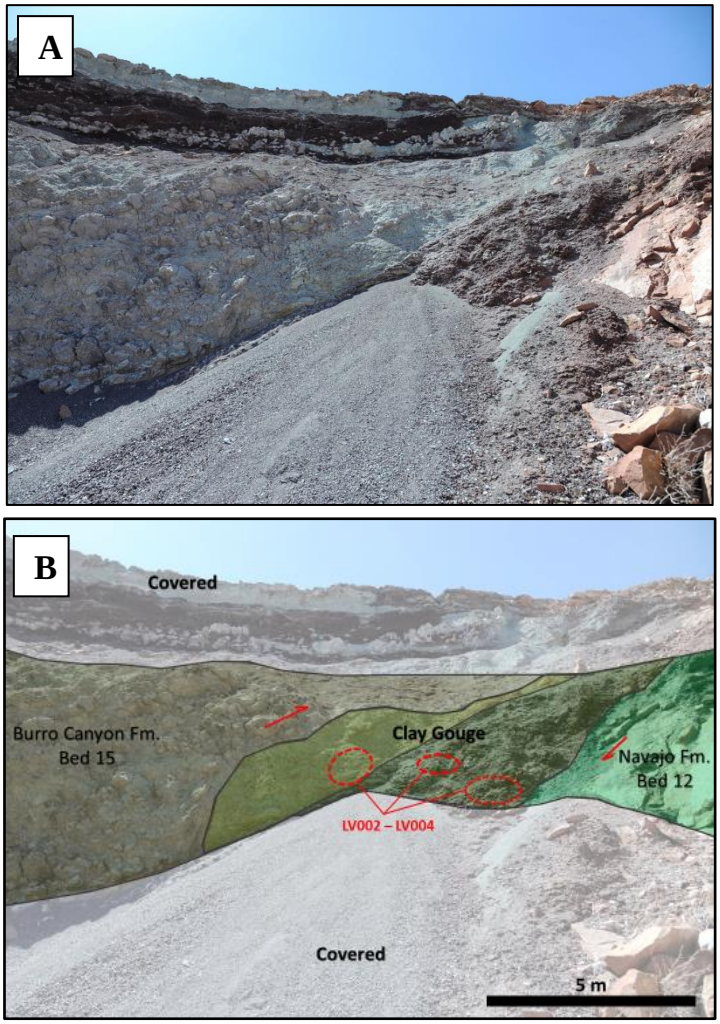

Fig 5. – Sample site 2 (LV002-LV004). Large damage zone and gouge zone with deep red clays. Footwall with great slicken lines.

Sandstone Formation (Jn) is juxtaposed against highly deformed Burro Canyon formation in the handing wall. The LVF at this site has the most offset with 400 meters. The main fault gouge at this location is divided into two distinct bands, one bleached and relatively coarse grained, and the other not bleached and more clay rich. The cumulative thickness of these two subzones is ~ 5 meters with the bleached zone accounting for ~1.25 meters of this. Samples were gathered from both subzones separately. The Navajo Sandstone at this site in not heavily altered of fractured, whereas the Burro Canyon Formation is highly fractured and altered. Sample LV002 through LV004 were collected from this site.

Sample location three is in the main active mining pit to the east of site two (Fig. 7). The gouge in this location was a bleached white-green to yellow with a more sandy texture than previous samples. The sample site is along the more minor Keystone fault within the pit. The gouge zone and alteration zone were less distinct than other sites due to overall heavy alteration. The zone with the heaviest alteration/gouge for this site was determined to be ~3 meters and the damage zone extended to as far as the exposure was visible, roughly 10 meters. The Keystone fault in this location has the lower Burro Canyon Formation in the footwall and the upper Burro Canyon formation in the hanging wall. The Keystone fault shows roughly 30 meters of displacement in this location. Samples LV005 and LV007 were taken from this site for analysis.

Sample site four is located to the east outside of the active mining location down the

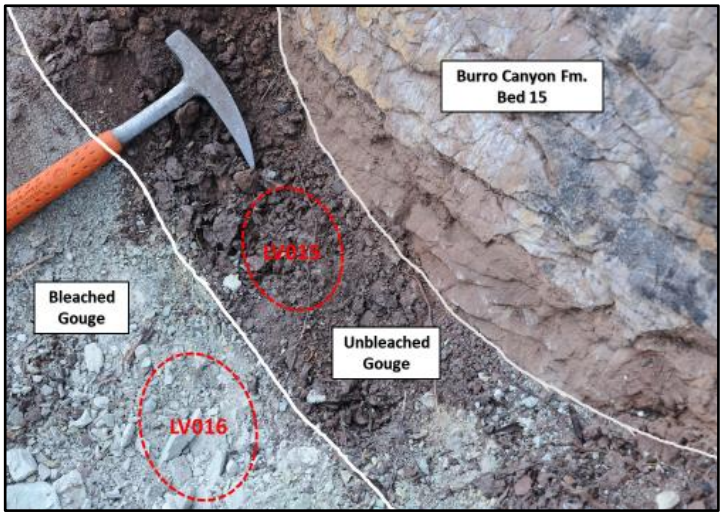

Fig 6 - Location 5 (LV015/LV016) showing variation of texture and color of clay gouge. Typical example of gouge composition separation.

Fig 7 – Sample site 3 (LV005-LV007). Heavily altered in both headwall and footwall. Gouge zone was the most clay rich area with little to no intact strata.

Fig 8 – Sample sites 4 (LV008-LV014) and 5 (LV015-LV016). Small fault exposure with obvious gouge and damage zones. Large lateral trench at site 4.

valley along the GTO fault (Fig. 7). The GTO fault at this site exhibits 150 meters of offset. This site is on land the has been leased by the mining company for future exploration. The process of sampling at this exposure required a lateral trench to be dug to uncover the gouge zone and remove surface alteration. This location had the largest number of subzones within the fault core. Five distinct zones were identified and sampled, LV008 to LV014. These samples stretched a 5.5-meter area bounded by damaged/fractured outcrop of Burro Canyon formation in the hanging wall and the Salt Wash member of the Morrison Formation in the footwall. The gouge at this location again ranged from bleached and dark red. Unique to this location zones alternated from coarse lithology to clay-rich back to coarse on a submeter interval.

The final sample area, location five in the Lucky Strike prospect (Fig. 6, Fig. 8) has

two separate locations grouped into one due to proximity. This site is located directly above (~5 m) location four on the GTO fault. The reason the site was chosen was because the vast differing lithology in gouge from the location only a few meters away. The gouge at this site had two distinct zones, a red subzone adjacent to bleached yellow zone (Fig. 6). The two zones were abutting the hanging wall of Burro Canyon Formation and the footwall again was the Morrison Formation. The total sampled zone was less than 1 meter across. The total fault core was ~ 5 meters but has been heavily weathered due to extensive surface processes. A total of four samples, two from each sublocation, were collected, LV008 through LV014 from the lower location and LV015 and LV016 from above.

X-Ray Diffraction (XRD)

Basic mineralogy of each sample was determined using randomly oriented powdered X-ray diffraction (XRD). This method requires a very fine grain powder < 4 µm in size to accurately assess the mineralogy by measuring the intensity and angle at which a mineral's crystal lattice refracts x- rays. Achieving this required extensive sample preparation. Each sample was crushed to a powder using an agate mortar and pestle. The powder was buffered with deionized water to avoid any alteration during the powdering process. Samples were then air-dried and sieved at 4 µm to ensure the elimination of interference from large grain diffraction. After completing preparation, samples were packed into random oriented pucks and loading into the Rigaku MiniFlex XRD. The scanning conditions for all samples were held consistent at 15 mA and 20 kV scanning from 3°-90°. Random orientation was chosen over an oriented scanning method because some peaks that are signature of some clays can be absent in oriented samples.

Accompanying this XRD work was Reitveld Refinement Modeling performed by Jason Kirk at the University of Arizona. Reitveld refinement is an extremely advanced method of XRD modeling that requires advanced size and density separation and characterization of peaks that is beyond the ability of this research lab. The results of Reitveld refinement is a bulk composition of the exact percent species for each mineral in a sample.

Computer Fault Modeling

A key tool used in this investigation was computer fault modeling. The selected program is a software package developed by Badleys known as T7. This is a 3D program that can be used to interpret, validate, build, and model fault seal potentials among many other features (Fig. 9). For this research, Badley's T7 software package was used for three main model types: shale gouge ratio modeling (SGR), fault seal capacity, and fault permeability. SGR is a mathematic function that simply calculates the percent of shale or clay in a faulted interval. This is shown as the amount of shale/clay that has passed a point as a set of strata is progressively faulted. The result is a triangle diagram showing relative percent of shale in the produced gouge based on where you are in the stratigraphic section. Along with SGR, fault seal and permeability modeling were also conducted. Both models consider the composition of stratigraphy as well as depth when faulted to determine permeability of a fault surface as well as the fault's ability to act as a barrier between each side (seal). Running any of these models required an understanding of the stratigraphy within the study area. More importantly, we needed to develop a pseudo V-Shale log, or a log of the volume and location of shale intervals within the study area's stratigraphy. This is the most important input into T7 for these models. The results of these three models were integrated with shallow well data and XRD data

about clay content all with the goal to understand the affects these gouges have on fluid movement of all types.

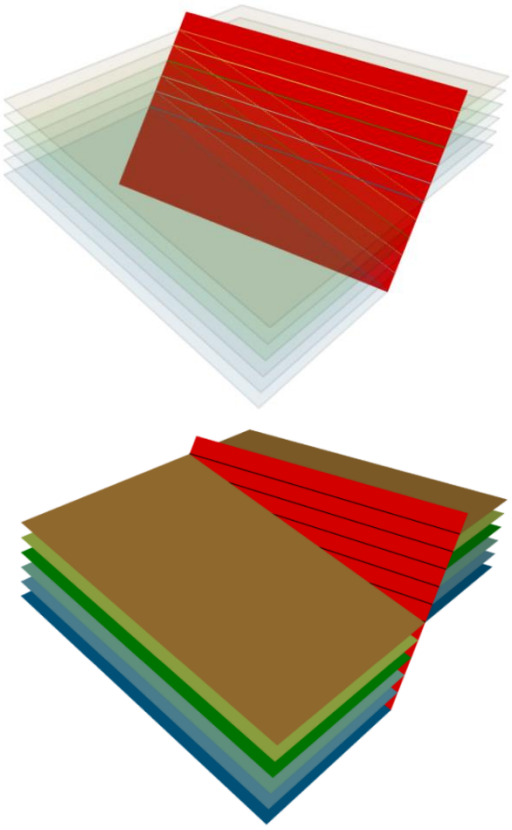

Fig. 9 – Schematic showing the function of triangle plots used for modeling. Relationship is show for each bed as it progressively is faulted through the stratigraphic section.

Results

Mineralogy of Clay Gouge

Randomly oriented powdered XRD results show high intensities of illite, quartz and kaolinite (Fig. 10). Along with major constituents, smaller concentrations of hematite, potassium feldspar, muscovite, and calcite were identified in select samples.

Findings from this XRD work show the overall composition of the gouge zones. While percent abundance of each mineral is not

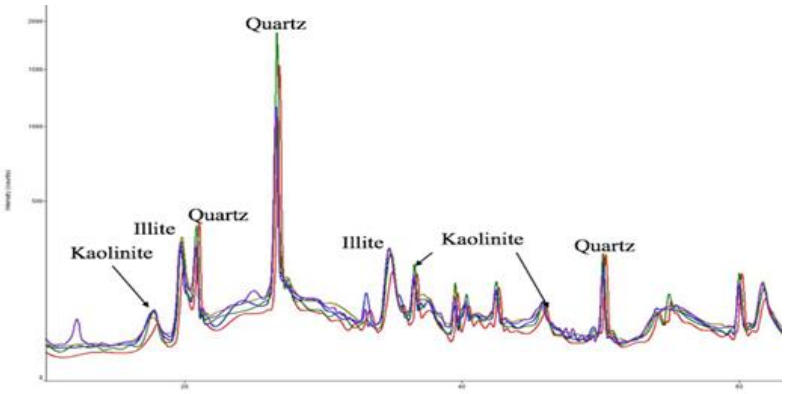

Fig. 10 – Random oriented powder x-ray diffraction of the main sample types found in Lisbon Valley.

calculated with this method, Rietveld models agree with the overall mineralogic trends found by randomly oriented powder XRD work. Rietveld modeling for three samples in Lisbon Valley was performed by Jason Kirk at University of Arizona. Modeling was performed on 3 size fractionations, 2-1 µm, 1-0.2µm and <0.2µm. The samples chosen were from the Lisbon Valley Fault (LV002), Keystone Fault (LV007), and the GTO Fault (LV012) (Fig. 10). Illite is the dominant mineral for the samples from the Lisbon Valley fault (LV002) at 69.3% in the 2-1µm, 90.97% in the 1-0.5 µm and 96.47% in the <2 µm size separations (Fig 11 and 13). The GTO fault sample (LV012) showed similar composition with illite as the dominant mineral with 72.06% in the 2-1µm, 73.75% in the 1-0.5 µm and 93.78% for the <2 µm size separations. (Fig 10). However, for sample LV007 on the GTO fault, quartz is the dominant mineral for the 1-0.5 µm separation with 44.09%, but illite becomes dominant in the 1-0.5 µm and <2 µm separation with 55.8% and 90.92% respectively (Fig. 11).

The mineral abundance for all samples in the <0.2µm separation show high percent of illite ranging between 90 and 95% (Fig 11). For samples LV002 and LV012 illite is the most abundant mineral followed by quartz at 14.16% and 9.91% respectively. LV007 is the only sample with high kaolinite concentrations at any

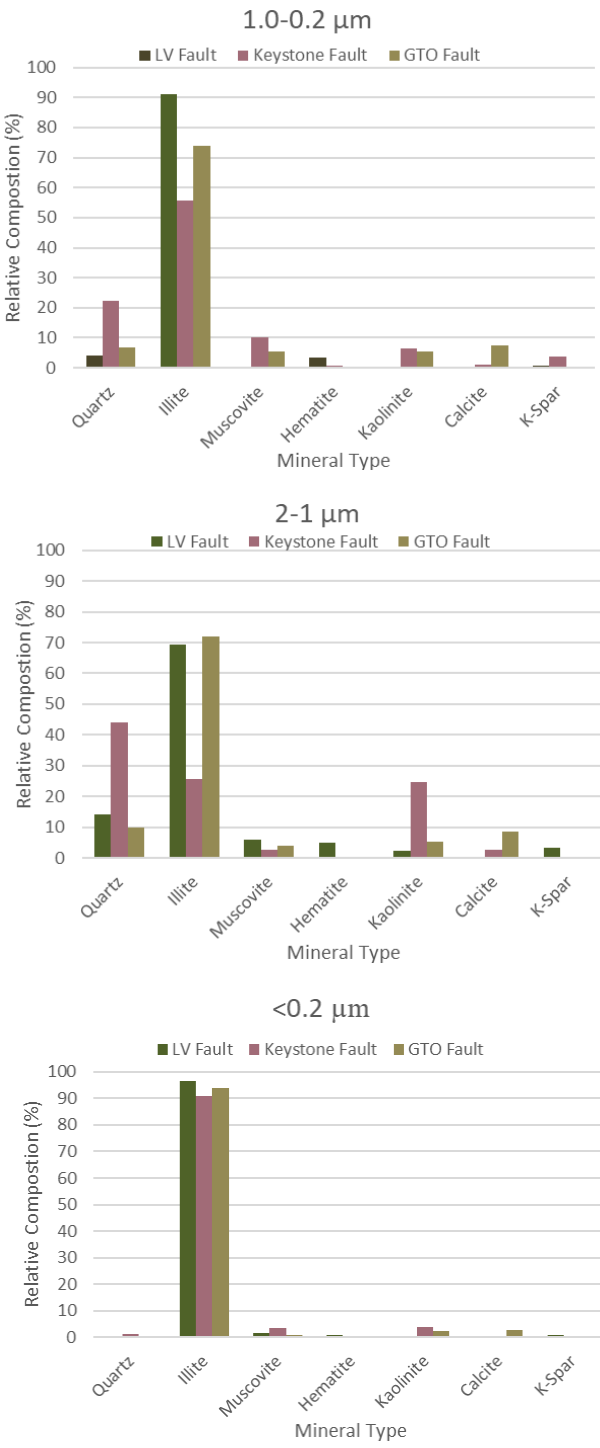

Fig. 11 – Three size fractionations and their relative mineral abundances. Size separations are the result of Reitveld modeling. Standard procedure is 4 size separations, this analysis is missing 1-0.2 µm because LV012 had a lack of this grade.

size separation with 24.5% and the lowest illite

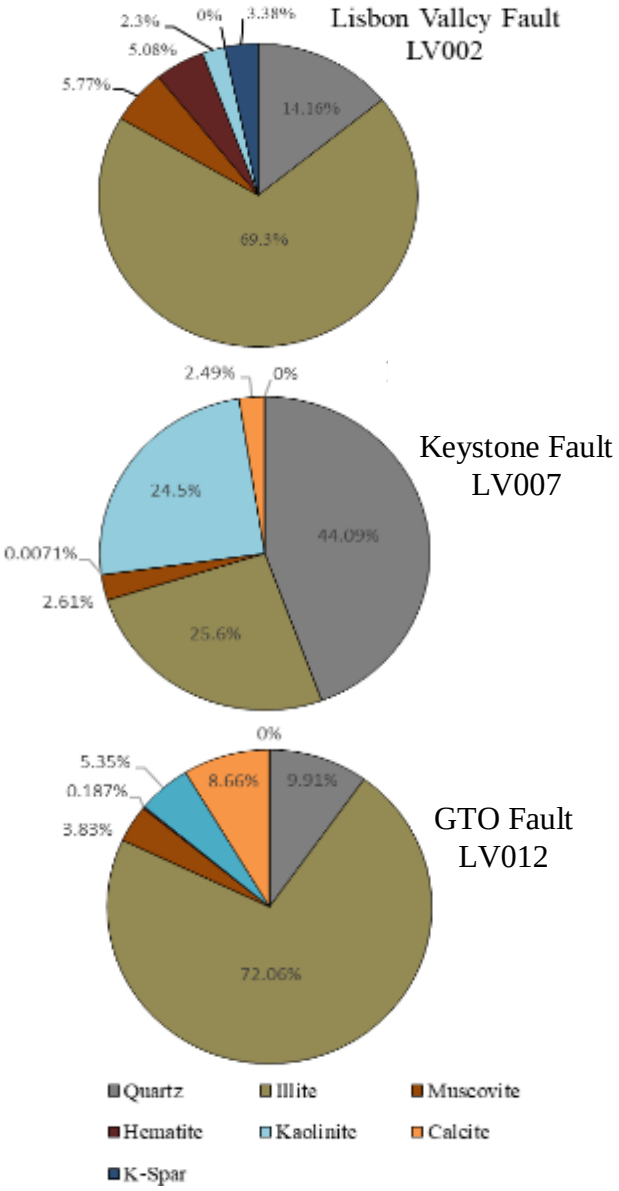

Fig. 12– Three samples from three faults, LV002 (LV Fault), LV007 (Keystone Fault), and LV012 (GTO Fault). Relative abundance of minerals within each sample. XRD data from Jason Kirk at the University of Arizona.

percentages of all the samples at 25.6%. LV002 has total composition is 70% clay minerals, while LV007 has 50% clays, and LV012 has roughly 80% clay minerals. This is consistent throughout all the size fractionations (Fig. 11).

LVF	Quartz	Illite	Muscovite	Hemetite	Kaolinite	Calcite	K-Spar
1-2 um	14.16	69.3	5.77	5.06	2.3	0	3.38
1-0.2 um	4.07	90.97	0.53	3.39	0.421	0	0.61
<0.2 um	0.04	96.47	1.72	0.778	0.211	0	0.76

Keystone	Quartz	Illite	Muscovite	Hemetite	Kaolinite	Calcite	K-Spar
1-2 um	44.09	25.6	2.61	0.0071	24.5	2.49	0
1-0.2 um	22.13	55.8	10.26	0.673	6.41	1.1	3.62
<0.2 um	1.13	90.92	3.34	0.178	3.8	0.589	0.042

GTO	Quartz	Illite	Muscovite	Hemetite	Kaolinite	Calcite	K-Spar
1-2 um	9.91	72.06	3.83	0.187	5.35	8.66	0
1-0.2 um	6.7	73.75	0.245	0.245	5.52	7.54	0.204
<0.2 um	0.19	72.53	0.11	0.11	2.31	2.8	0.008

Fig. 13 – Three size separations; 1-2um, 1-0.2um, and <0.2um. Shows distribution of each mineral in the gouge as a function of grain size.

Fault Property Modeling

Fault property modeling using T7 was performed for all sample sites through the whole stratigraphic section. Shale Gouge Ratio modeling is the first order technique used to predict the amount of shale/clay in the gouge (Fig. 14). Modeling indicates that samples LV015 and LV016 have the highest gouge ratio of 0.66. Samples LV008 through LV014 have the second highest values 0.54, followed by LV002-LV006 with 0.52, then LV001 at 0.37 and LV007 with 0.21.

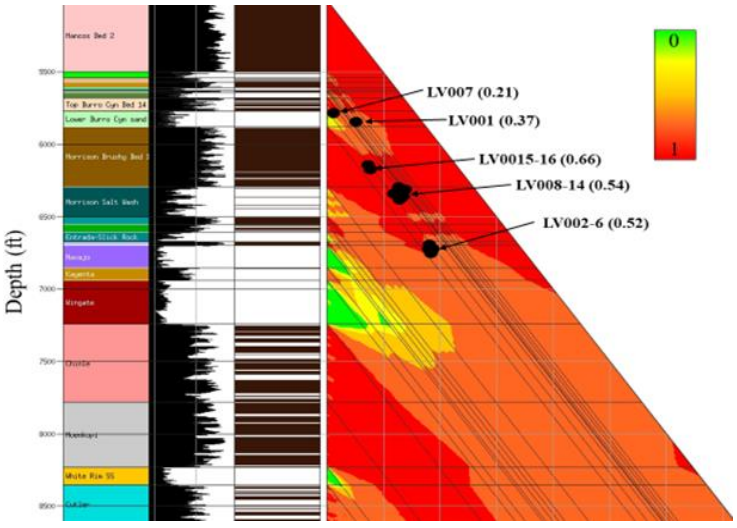

Fig. 14 - Shale Gouge Ratio (SGR) Values range from 0-1, 1 being 100% shale 0% being 100% clean sand/no shale. SGR is a mathematical function using shale bed thickness and dividing by fault throw.

A secondary modeling method to determine fault zone permeability properties was then conducted; this model uses a database of tested and known permeability values along with their associated stratigraphy and SGR. This model results in best fit values or a site along the faults based on SGR and previously known values. Like SGR, fault zone permeability models show a range of vales that are all very poor. This model shows poor permeability where SGR is high (LV015 and LV016) and highest permeability exists where SGR is the lowest at LV007 and LV001 (Fig 15).

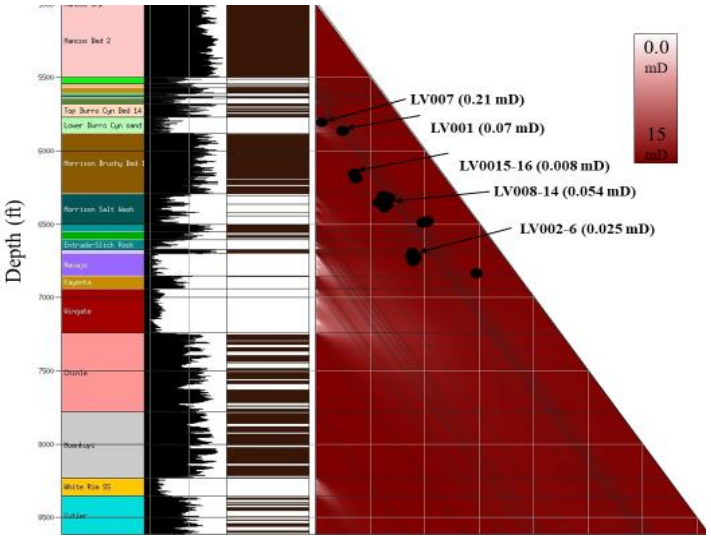

Fig. 15 - Fault permeability model (look-up), values range from 0 mD to 15 mD.

Lastly, a fault seal capillary pressure model was run to determine the amount of pressure the fault gouge is about to isolate. This model is again based off the original V-Shale log and SGR calculations. The fault results for seal potential models aligned with what was expected given the results from SGR and permeability models (Fig. 16). Like expected, sample sites with high SGR and low permeability exhibited higher relative fault seal potential (LV015 and LV016), while sites with low SGR and high permeability result in low fault seal potentials (LV007).

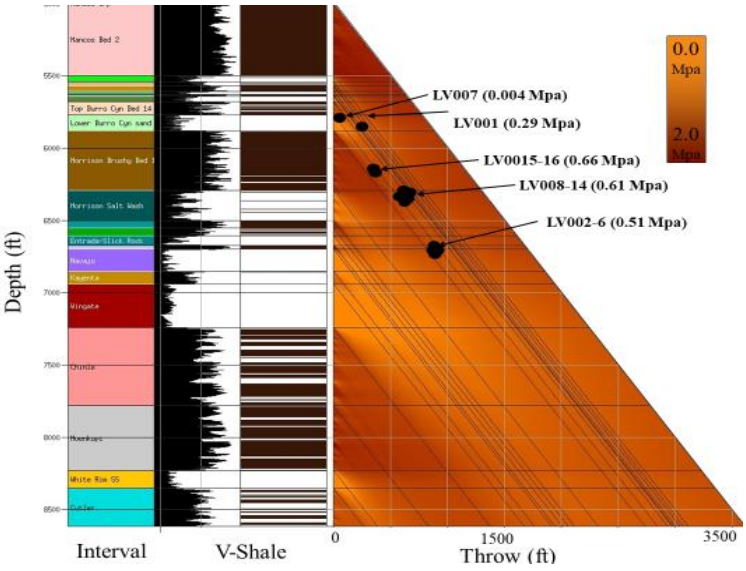

Fig. 16 - Threshold Capillary pressure model (Yeilding). Predicts range of entry pressures (Mpa) for fault gouge based on SGR models.

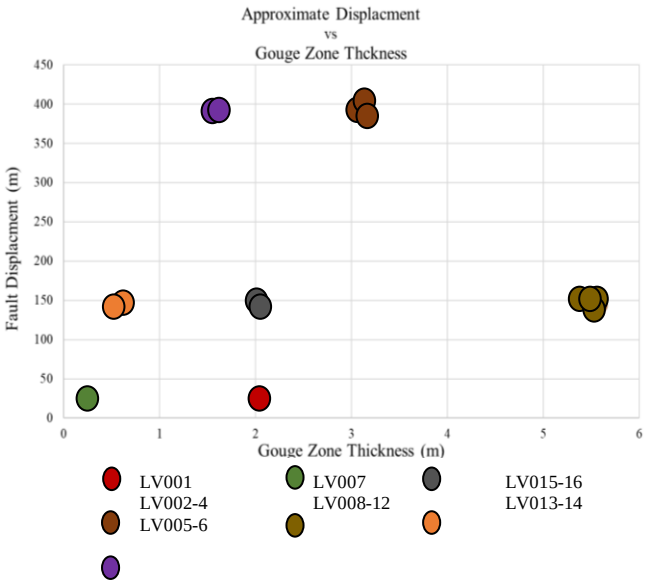

Fig. 17 – Cross plot of fault displacement against observed gouge zone widths for each sample site. Data shows no correlation between these two variables.

Discussion

Several relationships are possible between the individual factors observed in this study. Some of these factors contribute greatly to the overall configuration of gouge zones in the Lisbon Valley area. The following discussion highlights the most apparent of these.

Gouge Zone Geometry

This study has shown that all sampled sites have unique configurations and architectures. Some of the differences will help gain an understanding of this topic while some are less significant. The five most critical topics are the relationships concerning fault gouge zone geometry and offset, physical properties and lithology, mineralogy and physical properties, fault modeling and physical properties, and timing of clay within Lisbon Valley.

Gouge zones ranged from less than a meter to multiple meters in width, and fault displacement ranged from less than 10 meters to 100's of meters. However, these attributes do not tend to correlate (Fig. 17). This lack of correlation between fault gouge width and fault displacement is likely due to the location of the sample sites within the stratigraphic section. Another contribution to this relationship is likely a function of the original fault geometry and evolution. For example, LV007 is along the low offset (30 m) Keystone fault and has an observed gouge zone of only 0.2 meters in width. The stratigraphy that was involved in this

Sample Site	Color	Texture	Grainsize	Consolidation
LV001	Green to Yellow/Pale	Very clay rich, little sand	Medium	Poor to Medium
LV002 - LV004	Red to Green Pale/Buff	Clay/silt little sand	Fine to upper fine	Very Poor to Poor
LV005 - LV006	Red to Deep Maroon	Mostly clay some silt	Fine	Poor to Medium
LV007	Green, Yellow Pale/Buff	Sand to Silt/Clay Very chunky	Medium to Coarse	Very Well
LV008 - LV012	Red/Maroon to Green Pale /Buff	Majority clay with minor silt and sand	Fine to Medium	Very Poor to Poor
LV013 - LV014	Purple to Deep Maroon	Sand to Silt/Clay Mixed with soild rock	Fine to Upper Fine	Very Well to Medium
LV015 - LV016	Red to Deep Maroon	Clay with some Silt	Upper Fine to Medium	Well to Medium

Fig. 18 – Table of physical properties examined during sampling process.

fault was the sand rich lower Burro Canyon Formation and sandy/silty upper Burro Canyon Formation. These two lithologies are relatively sandy and therefore do not have very soft intervals that would be easily contributed to the gouge zone. On the other hand, LV001 is along a fault with similar displacement but occurring in a different portion of the stratigraphy that includes softer, shale-rich intervals. This lithological difference can be a determining factor in fault gouge widths. However, this relationship between lithologic type and formation of gouge zone width is violated in some sample sites in this study. For example, LV013 is hosted within an interbedded shale and sandstone deposit having a small gouge zone of roughly half a meter and fault displacement of 150 meters. On the other hand, LV008-LV012 is hosted within the same lithology yet has a 5.5-meter gouge zone.

Physical Gouge Properties

During the sampling process a detailed log of physical properties was taken. Some attributes that were logged were texture, grain size, color, and consolidation (Fig. 18). These observations revealed a correlation between the dominant color of the gouge and the stratigraphy involved in the faulting. A specific example of this is LV001 and LV007. These two sites are along faults that displace beds that are dominantly sandy and bleached. This bleaching process has mobilized the iron leaving the beds buff/pale to green in color. The displacement of the faults is such that these are contributing beds to the gouge. The resulting gouge represents this relationship in its color. Similarly, samples LV008 – LV012 are taken along the GTO fault where displacement is limited to the lower most Burro Canyon Formation and the Salt Wash Member of the Morrison Formation. The Morrison Formation in this area is an extensively iron stained red/maroon, siltstone to shale. This relationship between gouge color and related lithologic properties is observable throughout the sample locations. However, zoning of clay color within the fault gouge may be attributed to post-movement fluid alteration.

Another correlation found in the physical properties is the relationship between grain size and fault displacement (Fig. 19). A negative relationship was found that as the fault displacement increases, the average grain size of the fault gouge decreases. The most obvious example of this is in LV007. At this site, displacement on the Keystone fault was less than 30 m, and the grain size of the sample (0.425 mm) was like that of the surrounding Burro Canyon Formation. Similarly, sites with larger relative fault displacement (LV002-LV006) exhibit grain sizes that are finer than that of the surrounding lithology as expected. However, this relationship is interrupted by the lithology of the displaced rock. If the incorporated formations have a relatively small grain size prior to faulting, then the resulting fault gouge will have a smaller average grain size no matter the amount of displacement. LV001 is the example for this; fault offset here is minor, yet the grain size is very fine. This is due to the initial grain size of the rock.

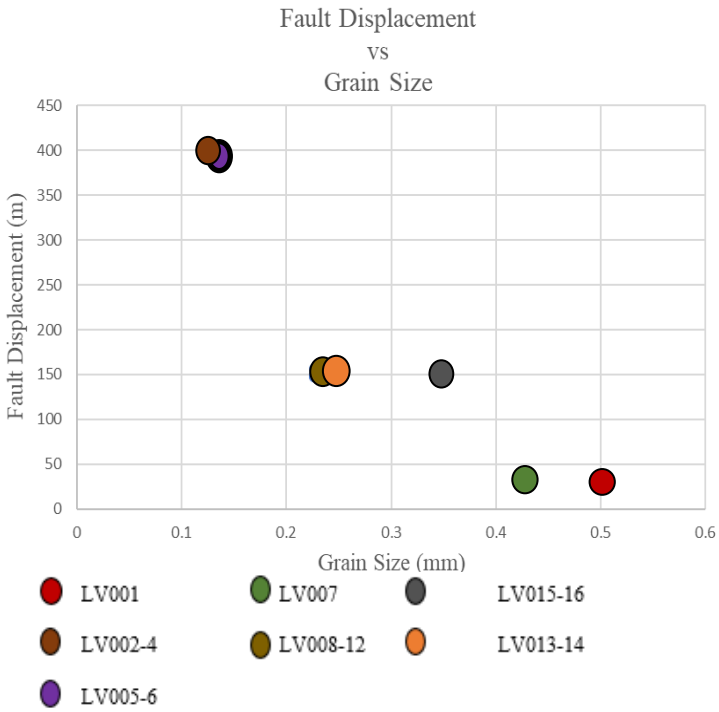

Fig. 19 – Cross plot of fault displacement against observed grain size for each sample site. Data shows no correlation betIen these two variables.

Mineralogy and Physical Properties

Three separate faults with distinct properties were tested for bulk composition. The result of Reitveld modeling reveals a relationship between mineral composition and physical properties. In sample LV007 most of this sample was quartz followed by two types of clay, illite and kaolinite. LV007 is the only sample that exhibited a high percent of quartz. The abundance of quartz can be seen in the physical features of the sample as well; LV007 was described as having medium to coarse grains and a chunky texture. The correlation between physical descriptions and mineralogical properties can be traced back the composition of the rock that was faulted. Like mentioned previously, the incorporated rock around the fault at LV007 is predominantly sand- and silt-rich stratigraphy. The correlation between mineralogy, grain size, and host lithology is obvious in LV007. However, the other two samples, LV008 and LV012, both have high percent of clays and lower quartz concentrations. This relates to the fine texture and small grain sizes of these samples as recorded in Figure 18. Composition of surrounding and incorporated stratigraphy contribute to the composition of these samples as well. Both sites respectively have stratigraphy that is rich in clay and silt; this is a major factor in the overall composition of the gouge.

Fault Zone Modeling

Another aspect of this project was computer modeling to predict Shale Gouge Ratio (SGR), permeability, and fault seal potential. Results of these models can be compared with bulk mineralogy of some of these samples to show an interesting relationship between SGR and mineralogy. This relationship is best observed in LV007; SRG models predicted a value of 21%, the lowest of all 16 samples (Fig. 10). A higher SGR translates to a higher overall clay/silt concentration within the gouge. Rietveld XRD modeling efforts identify quartz as the most abundant mineral in this sample at 45% along with the lowest overall clay proportions of any tested sample with only 50% (Fig. 12). The SGR models that predict a low shale/clay content at LV007 and are confirmed by the XRD results, meaning the sample with the lowest clay content was shown to also have the lowest SGR. In accordance to this, LV012 was modeled to have the highest proportions of clay with over 70% total clay content (Fig. 10). Again, the SGR model concurred and LV012 was predicted to have the highest SGR between these samples with 54% (Fig. 10). This result is predicted to hold true throughout the sample sites. Furthermore, fault permeability modeling indicates a similar relationship. LV007 is modeled to have the highest permeability at 0.21mD, meaning that there is a lack of clays to clog pore throats and reduce permeability (Fig. 15).

An important consideration in fault zones is the ability for a fault to either block or enable fluid flow along or across the fault's surface. The major contributing factor to this is the fault gouge itself. With the data that has been gathered for this research, a few predictions can be made about the fault seal potential within Lisbon Valley. It is commonly concluded that fault zones with SGR lower than 15% have little to no seal, faults with SGR between 15% and 18% are considered to have some seal potential, (<1 bar difference between adjacent fault blocks) and faults with SGR of over 20% are considered to have significant seal (Fristad, et al., 1997.). These values mean that given the SGR models produced in this study, every site that was sampled would be considered to have significant seal potential. The impact of these faults having high seal potential means that fluids that encounter these faults in the subsurface will not be transmitted though the fault zone. The lack of fluid

transmission means that ground water on opposite sides of a fault should have no or very little communication with each other depending on fault zone permeability and thickness. Understanding this segregation is tremendously important to the Lisbon Valley Mine while researching the possibility of pursuing in-situ recovery. Having a fully confined body of rock will allow this recovery effort to occur and understanding the fault's sealing potential is imperative to this effort.

Timing of Clay Enrichment

Most of copper mineralization in the valley is concentrated around major faults; the highest grades of ore are proximal to the faults with grade rapidly decreasing distally away from faults (Morrison and Parry, 1986). This spatial correlation indicates that mineral-rich fluids traveled along these faults during the hydrothermal mineralization process. The relationship between fault-focused mineralization and predicted seal potential contradict each other, which suggests that there were fewer clays during copper mineralization, and the fault zones have since been enriched later through argillic or authigenic processes. One piece of evidence for clay enrichment occurring after mineralization is that the gouge samples were not enriched with Cu, Pb, or Zn, the three most common metals in this type of fluid event (Solum et al., 2010). Given that these elements are not included within the gouge it is easy to assume that these clays were enriched at a later stage, post copper mineralization. This clay enrichment can be assumed to have since blocked the passage of fluids along most faults in Lisbon Valley. This assumption is backed by fault permeability and capillary pressure models. An alternative theory is that ore mineralization occurred while the faults were still active. Active faults have far less competency for seal and it would be likely that fluids would travel along them.

Conclusion

It is well known that faults have a control on the way fluids travel through the subsurface. However, not all faults behave the same way. A major factor in determining how fluids will be conducted when encountering a fault zone is the presence and configuration of the fault's interior, or gouge zone. Gouge is a fault rock the is typically rich in clay minerals. Clays are known to be barriers to fluid flow and can act as seals along fault planes.

This study concludes that clay-rich gouge zones were present in every observed fault zone around Lisbon Valley, ranging in thickness from ~20 cm to ~5.5 m. Fault gouge widths show no direct correlation to host fault offset while offset did tend to correlate with grain size. XRD analysis showed a strong correlation between host lithology and overall mineral constituents at all tested sites (LV002, LV007, and LV012). Similarly, the assumed relationship between mineralogy and the affect they would have on modeled fault properties was proven, meaning samples with higher the overall clay content of the sample resulted in a higher percent SGR and lower fault permeability.

Acknowledgments

Guidance from of my co-advisors Dr. Kim Hannula and Dr. Robert Krantz allowed for my project to evolve into a meaningful paper and taught me skills that I could not learn elsewhere. This research was made possible by the Lisbon Valley Mining Company allowing for collection of samples and access to land. Special thanks to Lantz Indergard and Brian Sparks at the mine for being so cooperative with and willing to share data. Reitveld refinement was performed by Jason Kirk at the University of Arizona and this study would not have been possible without his assistance. I would also like to acknowledge Fort Lewis College's

Undergraduate Research Foundation for providing funding to the research. Lastly, I would like to thank students who assisted in lab work, Ali Stapleton, Tanner Morgan, and Hayden Clay.

References

Chan, M.A., Parry, W.T., Petersen, E.U., and Hall, C.M., 2001, 40Ar/39Ar age and chemistry of manganese mineralization in the Moab and Lisbon fault systems, southeastern Utah: Geology, v. 29, p. 331, doi: 10.1130/0091-7613(2001)029<0331:aaaaco>2.0.co;2.

Crawford, B. R., Myers, R. D., Woronow, A., Faulkner, D. R. & Rutter, E. H., 2002. Porosity–permeability relationships in clay-bearing fault gouge. Paper 78214 presented at the Society of Petroleum Engineers/International Society of Rock Mechanics Conference, Iving Texas.

Davatzes, N.C., Eichhubl, P., and Aydin, A., 2005, Structural evolution of fault zones in sandstone by multiple deformation mechanisms: Moab fault, southeast Utah: Geological Society of America Bulletin, v. 117, p. 135, doi: 10.1130/b25473.1.

Engelder, J., 1974, Cataclasis and the generation of fault gouge: Geological Society of America Bulletin, v. 85, p. 1515-1522.

Fristad, X. Groth, X. Yielding G. and Freeman B., Quantitative fault seal prediction: a case study from Oseberg Syd: Hydrocarbon Seals: Importance for Exploration and Production, NPF Special Publication 7, pp. 107- 124. 1997.

Garden, I.R., Guscott, S.C., Burley, S.D., Foxford, K.A., Walsh, J.J., and Marshall, J., 2001, An exhumed palaeo-hydrocarbon migration fairway in a faulted carrier system, Entrada Sandstone of SE Utah, USA: Geofluids, v. 1, p. 195–213, doi: 10.1046/j.1468-8123.2001.00018.x.

Haines, S.H., and Pluijm, B.A.V.D., 2013, Corrigendum to Patterns of mineral transformations in clay gouge, with examples from low-angle normal fault rocks in the western USA" [Journal of Structural Geology 43 (2012) 2–32]: Journal of Structural Geology, v. 47, p. 52, doi: 10.1016/j.jsg.2012.11.007.

Leary, R.J., Umhoefer, P., Smith, M.E., and Riggs, N., 2017, A three-sided orogen: A new tectonic model for Ancestral Rocky Mountain uplift and basin development: Geology, doi: 10.1130/g39041.1.

Schmatz, J., Holland, M., Zee, W.V.D., and Urai, J.L., 2003, Fault Gouge Evolution in Layered Sand-Clay Sequences - First Results of Water-Saturated Sandbox Experiments: First EAGE International Conference on Fault and Top Seals - What do we know and where do we go?, doi: 10.3997/2214-4609.201405873.

Solum, J.G., Davatzes, N.C., and Lockner, D.A., 2010, Fault-related clay authigenesis along the Moab Fault: Implications for calculations of fault rock composition and mechanical and hydrologic fault zone properties: Journal of Structural Geology, v. 32, p. 1899–1911, doi: 10.1016/j.jsg.2010.07.009.

Solum, J.G., Pluijm, B.A.V.D., and Peacor, D.R., 2005, Neocrystallization, fabrics and age of clay minerals from an exposure of the Moab Fault, Utah: Journal of Structural Geology, v. 27, p. 1563–1576, doi: 10.1016/j.jsg.2005.05.002.

Walsh, J.J., Watterson, J., Heath, A.E., and Child, C., 1998, Representation and

scaling of faults in fluid flow models: Petroleum Geosciences, v., p. 241-251.

Morrison, S.J., and Parry, W.T., 1986, Formation of carbonate-sulfate veins associated with copper ore deposits from saline basin brines, Lisbon Valley, Utah: fluid inclusion and isotopic evidence: Economic Geology, v. 81, p. 1853-1866.